NASA Technical Memorandum 106679
ICOMP–94–13

IN-34
20305
29P

The Flux-Integral Method for Multidimensional Convection and Diffusion

B.P. Leonard
Institute for Computational Mechanics in Propulsion
Lewis Research Center
Cleveland, Ohio

University of Akron
Akron, Ohio

M.K. MacVean and A.P. Lock
Meteorological Office
Bracknell, Berkshire

August 1994

National Aeronautics and
Space Administration

INSTITUTE FOR COMPUTATIONAL MECHANICS IN PROPULSION
NASA
ICOMP
Lewis Research Center
Ohio Aerospace Institute

THE FLUX-INTEGRAL METHOD FOR MULTIDIMENSIONAL CONVECTION AND DIFFUSION

B.P. LEONARD
Institute for Computational Mechanics in Propulsion
Lewis Research Center
Cleveland, Ohio 44135

and

University of Akron
Akron, Ohio 44325–3903

M.K. MACVEAN and A.P. LOCK
Atmosphereic Processes Research Division
Meteorological Office, Bracknell, Berkshire, RG12 2SZ, U.K.

SUMMARY

The flux-integral method is a procedure for constructing an explicit, single-step, forward-in-time, conservative, control-volume update of the unsteady, multidimensional convection-diffusion equation. The convective-plus-diffusive flux at each face of a control-volume cell is estimated by integrating the transported variable and its face-normal derivative over the volume swept out by the convecting velocity field. This yields a *unique* description of the fluxes, whereas other conservative methods rely on nonunique, arbitrary pseudoflux-difference splitting procedures. The accuracy of the resulting scheme depends on the form of the *sub-cell interpolation* assumed, given cell-average data. Cellwise constant behaviour results in a (very artificially diffusive) first-order convection scheme. Second-order convection-diffusion schemes correspond to cellwise linear (or bilinear) sub-cell interpolation. Cellwise quadratic sub-cell interpolants generate a highly accurate convection-diffusion scheme with excellent phase accuracy. Under constant-coefficient conditions, this is a uniformly third-order polynomial interpolation algorithm (UTOPIA).

THE FLUX INTEGRAL

Consider the cell-average value of the transported scalar, $\bar{\phi}$, at a reference (central) cell, C. In two dimensions, an *exact*, single-step, explicit update can be written for the "new" (superscript +) cell value:

$$\bar{\phi}_C^{+} = \bar{\phi}_C + \text{FLUX}_w(i,j) - \text{FLUX}_w(i+1,j) + \text{FLUX}_s(i,j) - \text{FLUX}_s(i,j+1) \tag{1}$$

using standard index and compass-point notation. Note that this is strictly conservative in that the east-face convective-plus-diffusive flux of cell C, at (i,j), is identical to the west-face flux at $(i+1,j)$; similarly for the north- and south-face fluxes. In (1), the west-face flux, for example, is given by

$$\text{FLUX}_w(i,j) = \langle c_{xw}\,\phi_w \rangle - h \left\langle \alpha_w \left(\frac{\partial \phi}{\partial x}\right)_w \right\rangle \tag{2}$$

where the angle-brackets represent *time-averages* over Δt, and, assuming (for convenience) a uniform square mesh of side h, the west-face normal-component Courant number is

$$c_{xw} = \frac{u_w(t)\,\Delta t}{h} \tag{3}$$

and the west-face nondimensional diffusion parameter is written in terms of the (scalar) diffusivity, D_w, as

$$\alpha_w = \frac{D_w(t)\,\Delta t}{h^2} \tag{4}$$

with analogous definitions for the south face.

The convective contribution in (2) is equivalent to the total "mass" of ϕ swept through the west face along particle paths (or streamlines, in steady flow) over Δt. In principle, one could trace the particle paths backwards to the earlier time-level, for each face. This is shown, schematically, in Figure 1. Then the (exact) purely convective contribution is equivalent to integrating $\phi(x,y)$ *at the earlier time-level* over the area (or volume, in three dimensions) swept out by the particle paths:

$$\langle c_{xw}\,\phi_w \rangle = \iint_{\text{PPA}} \phi(x,y)\; \mathrm{d}(x/h)\; \mathrm{d}(y/h) \tag{5}$$

where PPA stands for particle-path area.

The flux-integral method now *approximates* (5) by replacing the particle-path area by the flux-integral parallelogram (FIP) by assuming the convecting velocity field to be locally constant (in both space and time) in the vicinity of the face in question. This is shown in Figure 2; note that the parallelogram is defined by the local (space-time-averaged) Courant number components, c_{xw} and c_{yw} (taken as both positive in the case shown). The flux-integral convective approximation is thus

$$\langle c_{xw} \phi_w \rangle \approx \iint_{\text{FIP}} \phi(x,y) \; d(x/h) \; d(y/h) \tag{6}$$

A similar approximation for the diffusive contribution results in

$$-h \left\langle \alpha_w \left(\frac{\partial \phi}{\partial x} \right)_w \right\rangle \approx -\frac{\alpha_w h}{c_{xw}} \iint_{\text{FIP}} \frac{\partial \phi}{\partial x} \; d(x/h) \; d(y/h) \tag{7}$$

where α_w is an appropriate average. If the ***sub-cell behaviour*** at the earlier time-level, $\phi(x,y)$, were known in complete detail, (6) would represent an *exact* flux due to pure convection by a constant velocity field. For non-zero diffusion, it turns out that (7) represents the diffusive flux to third order—provided the *sub-cell behaviour* is known in enough detail. The major task in the flux-integral method is thus an interpolation problem:

Given a set of cell-average values,
estimate sub-cell behaviour in an *accurate*
(and, ideally, *shape-preserving*) manner,
while observing the cell-average constraint:

$$\iint_{\text{cell}} \phi(x,y) \; d(x/h) \; d(y/h) = \bar{\phi} \quad \text{for all cells} \tag{8}$$

with an analogous formula in three dimensions.

For constant-density flow, the face-normal component Courant numbers used in constructing the flux-integral parallelograms should satisfy a discrete continuity equation for each cell:

$$c_{xw}(i,j) - c_{xw}(i+1,j) + c_{ys}(i,j) - c_{ys}(i,j+1) = 0 \tag{9}$$

Since the area of a flux-integral parallelogram is proportional to the face-normal Courant number component (e.g., the shaded area in Figure 2 is $c_{xw} h^2$), an initially constant scalar field will remain constant everywhere (to machine accuracy). This can be seen in Figure 3, where the sum of the "inflow areas" equals the sum of the "outflow areas" (irrespective of the local individual face-*transverse* Courant number components).

In the following sections, a number of different sub-cell interpolants are explored. A cellwise constant interpolant (locally equal to the cell average) results in a (very artificially diffusive) first-order convection scheme; modelled physical diffusion is absent, to a consistent order. This is not a viable scheme for practical CFD calculations. But, because of its simplicity, it is instructive to explore the flux-integral method in this case. Bilinear *downwind*-weighted sub-cell interpolation results in a two-dimensional analogue of the Lax-Wendroff scheme [1]. A cellwise quadratic interpolant over each cell generates a convection-diffusion scheme that is formally third-order accurate under constant-coefficient conditions. These three methods are briefly compared using the well-known "rotating hill" test problem.

FIRST-ORDER CONVECTION

Fluxes will be calculated for the west face of cell *C*. Entirely analogous fluxes for the south face can be written down using appropriate (x,y) permutations. Unless otherwise noted, the Courant number components will be taken as both positive. Referring to Figure 4, the west-face convective flux integral corresponding to (6) is seen to consist of three parts

$$\mathrm{FLUX}_w(i,j) \;=\; I_1 - I_2 + I_3 \tag{10}$$

where I_1 is the integral over the *rectangular* area, 1246, in cell *W*; I_2 is over the *triangular* area, 123, in cell *W*; and I_3 is over a similar triangular area, 456, in cell *SW*. Assuming ϕ to be cellwise constant (equal to the respective cell average), the integrals in (1) are proportional to the respective areas times the local cell-average value. This gives

FIRST-ORDER FIM:

$$\mathrm{FLUX}_w(i,j) \;=\; c_{xw}\,\bar{\phi}_W - \frac{c_{xw}c_{yw}}{2}\,\bar{\phi}_W + \frac{c_{xw}c_{yw}}{2}\,\bar{\phi}_{SW} \tag{11}$$

or, on rearrangement,

$$\text{FLUX}_w(i,j) = c_{xw}\left[\bar{\phi}_W - \frac{c_{yw}}{2}(\bar{\phi}_W - \bar{\phi}_{SW})\right] \tag{12}$$

The term in square brackets can be considered to be the effective average convected face value. Note that it consists of the one-dimensional, first-order upwind (''donor-cell'') value, $\bar{\phi}_W$, modified by a *transverse-gradient* term proportional to the transverse Courant number component at the face. It should be clear how the formula changes for other combinations of signs of c_{xw} and c_{yw}. To a consistent order, there is no (physical) diffusive flux, since cellwise constant behaviour implies a zero-gradient within each cell.

Substituting (12), and the analogous formula for FLUX_s, into (1) gives an overall (constant-coefficient) convective update equation:

$$\bar{\phi}_C^{+} = \bar{\phi}_C - c_x(\bar{\phi}_C - \bar{\phi}_W) - c_y(\bar{\phi}_C - \bar{\phi}_S)$$
$$+ c_x c_y(\bar{\phi}_C - \bar{\phi}_W - \bar{\phi}_S + \bar{\phi}_{SW}) \tag{13}$$

This is identical to a semi-Lagrangian update [2], using *bilinear* interpolation around the departure point, collocated at *node* values: $\bar{\phi}_C$, $\bar{\phi}_W$, $\bar{\phi}_{SW}$, and $\bar{\phi}_S$ (located at the centroids of the respective cells). [For cellwise constant, linear, or bilinear interpolants, node values are equal to the respective cell-average values. This is *not* the case for higher-order interpolants.]

Using an appropriate upwinding strategy for other convecting velocity directions, it is not hard to show that the von Neumann stability condition for this scheme is given by a square region in the (c_x, c_y) plane:

$$|c_x| \le 1 \quad \text{and} \quad |c_y| \le 1 \tag{14}$$

SECOND-ORDER METHODS

Second-order convection-diffusion methods result from assuming cellwise linear or bilinear sub-cell behaviour. In this case, it is convenient to introduce local, normalised coordinates in cell W:

$$\xi = \frac{x}{h} - (i - 1) \tag{15}$$

and

$$\eta = \frac{y}{h} - j \tag{16}$$

as shown in Figure 5. Note that the central cell, C, is located at (i,j). The top of the flux-integral parallelogram is represented by

$$\eta_{top}(\xi) = 0.5 + \frac{c_{yw}}{c_{xw}} (\xi - 0.5) \tag{17}$$

A general bilinear sub-cell interpolant within cell W takes the form

$$\phi(\xi, \eta) = C_1 + C_2 \xi + C_3 \eta + C_4 \xi \eta \tag{18}$$

The cell-average constraint, (8), implies

$$C_1 = \bar{\phi}_W \tag{19}$$

The slope-constants, C_2 and C_3, and the twist-constant, C_4, can be chosen in a number of different ways. For example, a two-dimensional analogue of Fromm's method [3] results from choosing

$$C_2 = \frac{1}{2} \left(\bar{\phi}_C - \bar{\phi}_{WW} \right) \tag{20}$$

$$C_3 = \frac{1}{2} \left(\bar{\phi}_{NW} - \bar{\phi}_{SW} \right) \tag{21}$$

and

$$C_4 = 0 \tag{22}$$

Note that this represents a symmetrical distribution with respect to cell W, independent of velocity direction. Upwind or downwind weighting can also be used. In the interest of brevity, only one scheme will be considered here in detail. This is based on downwind-weighted *bilinear* interpolation. For example, throughout cell W, the interpolant is collocated (for c_{xw}, $c_{yw} > 0$) at *node values*: $\bar{\phi}_C$, $\bar{\phi}_N$, and $\bar{\phi}_{NW}$ (in addition to $\bar{\phi}_W$). This turns out to be a two-dimensional generalisation of the Lax-Wendroff method. For positive Courant number components, the interpolant within cell W is

$$\phi(\xi,\eta) = \bar{\phi}_W + (\bar{\phi}_C - \bar{\phi}_W)\,\xi + (\bar{\phi}_{NW} - \bar{\phi}_W)\,\eta$$
$$+ (\bar{\phi}_N - \bar{\phi}_{NW} - \bar{\phi}_C + \bar{\phi}_W)\,\xi\eta \tag{23}$$

with a corresponding normal gradient, within cell W,

$$\frac{\partial\phi}{\partial\xi} = (\bar{\phi}_C - \bar{\phi}_W) + (\bar{\phi}_N - \bar{\phi}_{NW} - \bar{\phi}_C + \bar{\phi}_W)\,\eta \tag{24}$$

Using local, cell-centered coordinates, similar formulae hold for each cell; in particular, cell *SW* formulae can be obtained from (23) and (24) by shifting all indexes "south" by one unit in (16), (23), and (24).

As before, the convective flux integral is split into three geometrically distinct parts. In this case,

$$I_1 = \int_{0.5-c_{xw}}^{0.5}\left[\int_{-0.5}^{0.5} \phi(\xi,\eta)\,\mathrm{d}\eta\right]\mathrm{d}\xi \tag{25}$$

$$= \int_{0.5-c_{xw}}^{0.5}\left[\bar{\phi}_W + (\bar{\phi}_C - \bar{\phi}_W)\,\xi\right]\mathrm{d}\xi \tag{26}$$

$$= c_{xw}\bar{\phi}_W + \left(\frac{c_{xw} - c_{xw}^2}{2}\right)(\bar{\phi}_C - \bar{\phi}_W) \tag{27}$$

When rearranged as

$$I_1 = c_{xw}\left[\frac{1}{2}(\bar{\phi}_C + \bar{\phi}_W) - \frac{c_{xw}}{2}\,(\bar{\phi}_C - \bar{\phi}_W)\right] \tag{28}$$

this will be recognised as the *one-dimensional* Lax-Wendroff flux [3]. The second (negative) contribution over the triangular area in cell *W* is

$$-I_2 = -\int_{0.5-c_{xw}}^{0.5}\left[\int_{\eta_{top}(\xi)}^{0.5} \phi(\xi,\eta)\,\mathrm{d}\eta\right]\mathrm{d}\xi \tag{29}$$

Using (17), this becomes, after some rearrangement,

$$
-\bar{I}_2 = -c_{xw}c_{yw}\begin{bmatrix} \frac{1}{8}(\bar{\phi}_C + \bar{\phi}_W + \bar{\phi}_N + \bar{\phi}_{NW}) \\ -\frac{c_{xw}}{6}(\bar{\phi}_N + \bar{\phi}_C - \bar{\phi}_{NW} - \bar{\phi}_W) \\ -\frac{c_{yw}}{12}(\bar{\phi}_N + \bar{\phi}_{NW} - \bar{\phi}_C - \bar{\phi}_W) \\ +\frac{c_{xw}c_{yw}}{8}(\bar{\phi}_N - \bar{\phi}_{NW} - \bar{\phi}_C + \bar{\phi}_W) \end{bmatrix} \tag{30}
$$

Then, I_3 is obtained from I_2 by shifting all indices south by one unit.

The diffusive flux is computed in a similar way. In particular

$$
-\alpha_w\left(\frac{\partial\phi}{\partial\xi}\right)_{\text{avg}} = -\frac{\alpha_w}{c_{xw}}\iint_{\text{FIP}}\frac{\partial\phi}{\partial\xi}\,d\xi\,d\eta \tag{31}
$$

This is also conveniently split into three parts. In this case

$$
-\frac{\alpha_w}{c_{xw}}I_1 = -\alpha_w(\bar{\phi}_C - \bar{\phi}_W) \tag{32}
$$

which will be recognised as the classical, second-order, *one-dimensional* expression for the diffusive flux across the west face. But there are also contributions from transverse convective coupling. In particular,

$$
+\frac{\alpha_w}{c_{xw}}I_2 = \alpha_w\begin{bmatrix} \frac{c_{yw}}{4}(\bar{\phi}_N + \bar{\phi}_C - \bar{\phi}_{NW} - \bar{\phi}_W) \\ -\frac{c_{yw}^2}{6}(\bar{\phi}_N - \bar{\phi}_{NW} - \bar{\phi}_C + \bar{\phi}_W) \end{bmatrix} \tag{33}
$$

and the corresponding I_3 term is again obtained by shifting all indices south by one unit.

The total west-face convective-plus-diffusive flux is then

BILINEAR DOWNWIND:

$$\mathrm{FLUX}_w(i,j) = c_{xw} \left\{ \begin{array}{l} \frac{1}{2}(\bar{\phi}_C + \bar{\phi}_W) - \frac{c_{xw}}{2}(\bar{\phi}_C - \bar{\phi}_W) \\ - \frac{c_{yw}}{8}\left[(\bar{\phi}_N - \bar{\phi}_S) + (\bar{\phi}_{NW} - \bar{\phi}_{SW})\right] \\ + \frac{c_{xw}c_{yw}}{6}\left[(\bar{\phi}_N - \bar{\phi}_S) - (\bar{\phi}_{NW} - \bar{\phi}_{SW})\right] \\ + \frac{c_{yw}^2}{12}\left[(\bar{\phi}_N - 2\bar{\phi}_C + \bar{\phi}_S) + (\bar{\phi}_{NW} - 2\bar{\phi}_W + \bar{\phi}_{SW})\right] \\ - \frac{c_{xw}c_{yw}^2}{8}\left[(\bar{\phi}_N - 2\bar{\phi}_C + \bar{\phi}_S) - (\bar{\phi}_{NW} - 2\bar{\phi}_W + \bar{\phi}_{SW})\right] \end{array} \right\}$$

$$- \alpha_w \left\{ \begin{array}{l} (\bar{\phi}_C - \bar{\phi}_W) - \frac{c_{yw}}{4}\left[(\bar{\phi}_N - \bar{\phi}_S) - (\bar{\phi}_{NW} - \bar{\phi}_{SW})\right] \\ + \frac{c_{yw}^2}{6}\left[(\bar{\phi}_N - 2\bar{\phi}_C + \bar{\phi}_S) - (\bar{\phi}_{NW} - 2\bar{\phi}_W + \bar{\phi}_{SW})\right] \end{array} \right\} \qquad (34)$$

The interesting thing about this formula is that (referring to Figure 4) every term is face-centered in both x and y directions. In this case, the *downwind*-weighted sub-cell interpolation is "balanced" by the *natural upwinding* involved in the flux-integral calculation. The resulting convective-plus-diffusive flux is independent of velocity direction — just like the Lax-Wendroff method in one dimension. The overall update equation involves the square, nine-point stencil, centered on C. For pure convection at constant velocity, the update is identical to that of a semi-Lagrangian scheme using the same nine-point stencil.

Although the semi-Lagrangian convection scheme can be obtained from the flux-integral form, *the reverse is not true*. This is easily seen by writing out the complete update based on (34). Notice how the $c_x(c_x c_y)$ term from the east-west flux difference combines with the $c_y(c_x^2)$ term from the north-south flux difference. The purely convective von Neumann stability region is again the square, given by (14). Stability regions in the (c_x, c_y) plane for finite values of α are discussed elsewhere [4].

UNIFORMLY THIRD-ORDER POLYNOMIAL INTERPOLATION ALGORITHM

Assuming symmetrically weighted cellwise *quadratic* sub-cell interpolation within each cell leads to a uniformly third-order polynomial interpolation algorithm for convection and diffusion (under constant-coefficient conditions). In a variable (but solenoidal) convecting velocity field, with possibly variable diffusivity, the algorithm is no longer formally third-order accurate; however, the *practical* accuracy is significantly better than that of formally second-order schemes. Phase accuracy, in particular, is excellent — just as in the case of the corresponding one-dimensional QUICKEST scheme [5,6,7].

Within cell W, the quadratic interpolation takes the (velocity-direction-independent) form:

$$\begin{aligned}\phi(\xi,\eta) &= \bar{\phi}_W - \frac{1}{24}\left(\bar{\phi}_C + \bar{\phi}_{SW} + \bar{\phi}_{WW} + \bar{\phi}_{NW} - 4\bar{\phi}_W\right) \\ &+ \left(\frac{\bar{\phi}_C - \bar{\phi}_{WW}}{2}\right)\xi + \left(\frac{\bar{\phi}_C - 2\bar{\phi}_W + \bar{\phi}_{WW}}{2}\right)\xi^2 \\ &+ \left(\frac{\bar{\phi}_{NW} - \bar{\phi}_{SW}}{2}\right)\eta + \left(\frac{\bar{\phi}_{NW} - 2\bar{\phi}_W + \bar{\phi}_{SW}}{2}\right)\eta^2 \end{aligned} \tag{35}$$

Note that this satisfies the cell-average constraint, (8). Also note that the nodal value, ϕ_W, is not the same as the cell average; in fact,

$$\phi_W = \phi(0,0) = \bar{\phi}_W - \frac{1}{24}\left(\bar{\phi}_C + \bar{\phi}_{SW} + \bar{\phi}_{WW} + \bar{\phi}_{NW} - 4\bar{\phi}_W\right) \tag{36}$$

The x-direction gradient within cell W is

$$\frac{\partial\phi}{\partial\xi} = \left(\frac{\bar{\phi}_C - \bar{\phi}_{WW}}{2}\right) + \left(\bar{\phi}_C - 2\bar{\phi}_W + \bar{\phi}_{WW}\right)\xi \tag{37}$$

Convective Flux in the Absence of Diffusion

For pure convection, the west-face flux is computed in the usual way. As perhaps, by now, expected, the first component of the flux integral generates the one-dimensional (in this case, QUICKEST formula:

$$I_1 = c_{xw}\left[\frac{1}{2}\left(\bar{\phi}_C + \bar{\phi}_W\right) - \frac{c_{xw}}{2}\left(\bar{\phi}_C - \bar{\phi}_W\right) - \left(1 - \frac{c_{xw}^2}{6}\right)\left(\bar{\phi}_C - 2\bar{\phi}_W + \bar{\phi}_{WW}\right)\right] \tag{38}$$

Note the appearance of the upwind-weighted normal-curvature term (resulting from the natural upwinding inherent in the flux integral). Integration over the respective triangular areas in cells W and SW introduces several cross-difference terms. The final form of the purely convective flux is (referring to Figure 4):

QUADRATIC (CONVECTION):

$$\mathrm{FLUX}_w(i,j) = c_{xw}\left\{\begin{array}{l} \frac{1}{2}(\bar{\phi}_C + \bar{\phi}_W) - \frac{c_{xw}}{2}(\bar{\phi}_C - \bar{\phi}_W) \\ \qquad - \left(\frac{1 - c_{xw}^2}{6}\right)(\bar{\phi}_C - 2\bar{\phi}_W + \bar{\phi}_{WW}) \\ - \frac{c_{yw}}{2}(\bar{\phi}_W - \bar{\phi}_{SW}) \\ - c_{yw}\left(\frac{1}{4} - \frac{c_{xw}}{3}\right)(\bar{\phi}_C - \bar{\phi}_W - \bar{\phi}_S + \bar{\phi}_{SW}) \\ - c_{yw}\left(\frac{1}{4} - \frac{c_{yw}}{6}\right)(\bar{\phi}_{NW} - 2\bar{\phi}_W + \bar{\phi}_{SW}) \\ + c_{yw}\left(\frac{1}{12} - \frac{c_{xw}^2}{8}\right)\left[\begin{array}{l}(\bar{\phi}_C - 2\bar{\phi}_W + \bar{\phi}_{WW}) \\ - (\bar{\phi}_S - 2\bar{\phi}_{SW} + \bar{\phi}_{SWW})\end{array}\right] \\ + c_{yw}\left(\frac{1}{12} - \frac{c_{yw}^2}{24}\right)(\bar{\phi}_{NW} - 3\bar{\phi}_W + 3\bar{\phi}_{SW} - \bar{\phi}_{SSW}) \end{array}\right\} \quad (39)$$

It is instructive to identify the role played by each of these terms. The first three terms represent the one-dimensional (QUICKEST) contribution; note that all the remaining terms contain a c_{yw} coefficient. The fourth term in (39) is the *transverse gradient* that previously appeared in the first-order scheme. This is, in fact, a second-order term—just as is the *normal gradient* (second term). The fifth term represents *twist*, an interaction between normal and transverse convection. The next term is a *transverse-curvature* contribution. The final two terms in (39) are actually fourth-order contributions. Dropping these terms does not affect the formal (constant-coefficient) third-order accuracy of the overall update equation. However, they do affect the stability of the scheme. Without the higher-order terms, the purely convective stability region is *approximately* the diamond-shaped region

$$|c_x| + |c_y| < 1 \tag{40}$$

Including these terms (that arise naturally in the flux-integral formulation) results once again in the square stability region given by (14).

Third-Order Diffusive Flux

Applying the usual three-part-integral procedure to (37) results in the following diffusive flux:

$$-\alpha_w \left(\frac{\partial \phi}{\partial \xi}\right)_{avg} = -\alpha_w \left\{ \begin{array}{l} (\bar{\phi}_C - \bar{\phi}_W) - \frac{c_{xw}}{2}(\bar{\phi}_C - 2\bar{\phi}_W + \bar{\phi}_{WW}) \\ \\ - \frac{c_{yw}}{2}(\bar{\phi}_C - \bar{\phi}_W - \bar{\phi}_S + \bar{\phi}_{SW}) \\ \\ + \frac{c_{xw}c_{yw}}{3}\left[\begin{array}{l} (\bar{\phi}_C - 2\bar{\phi}_W + \bar{\phi}_{WW}) \\ -(\bar{\phi}_S - 2\bar{\phi}_{SW} + \bar{\phi}_{SWW}) \end{array}\right] \end{array} \right\} \tag{41}$$

The first term is the classical (one-dimensional) second-order first-difference across the face. The second, ***normal-curvature*** term, represents the effect of normal convection on the time-averaged normal gradient; this is a third-order convection-diffusion cross-coupling term that also appears in the one-dimensional QUICKEST formula [5]. The third, *twist*, term represents the coupling effect of *transverse* convection; this is a (two-dimensional) third-order term. The final term is actually a (partial) fourth-order cross-coupling term, kept, once again, because of enhanced stability properties [4].

Diffusive Contribution to the Convective Flux

The convection-diffusion coupling terms just described represent the effects of convection in estimating the diffusive flux. They arise naturally in the flux-integral formulation. For uniformly third-order consistency, one also needs to estimate the analogous cross-coupling effects of diffusion on the convective flux. Because of the assumed curvature in the sub-cell interpolation, diffusion changes the value of ϕ over Δt as it is being convected through a particular cell face. As shown in [8], this change is given by $(\alpha/2)\nabla^2\phi$. Performing the usual three-part flux-integral calculation leads to an *additional* diffusive contribution to the convective flux of the form

$$+ c_{xw} \left\{ \begin{array}{l} \dfrac{\alpha_{xw}}{2}\left[(\bar{\phi}_C - 2\bar{\phi}_W + \bar{\phi}_{WW}) + (\bar{\phi}_{NW} - 2\bar{\phi}_W + \bar{\phi}_{SW})\right] \\ - \dfrac{\alpha_w c_{yw}}{4} \left[\begin{array}{l} (\bar{\phi}_C - 2\bar{\phi}_W + \bar{\phi}_{WW}) - (\bar{\phi}_S - 2\bar{\phi}_{SW} + \bar{\phi}_{SWW}) \\ + (\bar{\phi}_{NW} - 3\bar{\phi}_W + 3\bar{\phi}_{SW} - \bar{\phi}_{SSW}) \end{array} \right] \end{array} \right\} \quad (42)$$

which must be added to (39) to give the total convective flux. The convective-plus-diffusive flux at the west face is thus the sum of (39), (41), and (42). A von Neumann stability analysis of the constant-coefficient overall update algorithm [4] shows that the useful region in (c_x, c_y, α) space is given, as a minimum, by the "cylinder":

$$|\mathbf{c}| \leq 1, \quad 0 \leq \alpha \leq 0.25 \quad (43)$$

Reference [4] also describes a simple and inexpensive (vectorisable) upwinding strategy based on the "generic stencil" technique, using FORTRAN functions NINT and SIGN.

CONVECTIVE TEST PROBLEM

The three schemes described here have been applied to the rotating Gaussian hill problem under purely convective conditions ($\alpha=0$). Details of the mesh, time-step, and other parameters are given in Reference [4]. Figure 6 shows the initial state in a superfine-grid rendering. The cell-average initial data is shown in Figure 7. Figure 8 shows the first-order results after one (anticlockwise) rotation. The "Lax-Wendroff" cell-average results are shown in Figure 9, with a close-up of the peak region, showing the sub-cell behaviour, in Figure 10. Figures 11 and 12 give the corresponding UTOPIA results. As mentioned before, the first-order scheme is far too artificially diffusive to even be considered for practical application. As in one dimension, the Lax-Wendroff-type scheme is excessively dispersive, showing significant phase-lag errors in the "wake". By contrast, UTOPIA has good accuracy and excellent phase behaviour, just as in the one-dimensional case [5,7].

Extensive other studies of purely convective and convective-diffusive test-problems at a number of grid-refinements have consistently shown the superiority of UTOPIA. Not surprisingly, it is more accurate than lower-order schemes. It is also more expensive — *per mesh point calculation.* The important conclusion, however, is that, *for a prescribed accuracy*, UTOPIA can be used on a much coarser mesh (with a concomitantly larger time-step) — *the overall cost is then much lower* than that of lower-order schemes.

CONCLUSION

The flux-integral method is a powerful technique for estimating convective-plus-diffusive fluxes in a strictly conservative formulation of an explicit, single-step update formula for the multidimensional convection-diffusion equation. The assumption of locally constant convecting velocities near each control-volume face means that the formal accuracy of the convection terms is at most second order — e.g., the convecting velocity field could be staggered in time by $\Delta t/2$ with respect to transported scalars. Variable diffusivity would typically be lagged, and therefore only first-order accurate in time. However, spatial accuracy is enhanced by using higher-order sub-cell interpolation. Under constant-coefficient conditions, an Nth-order sub-cell interpolation leads to an $(N+1)$th-order accurate convection-diffusion scheme — in both space and time.

Cellwise constant sub-cell interpolation leads to an unworkable (artificially diffusive) first-order convection scheme. Cellwise linear or bilinear interpolants generate second-order convection-diffusion schemes. Downwind-weighted bilinear interpolation gives a multi-dimensional analogue of the Lax-Wendroff scheme. However, because of the unsymmetrical weighting of the interpolant, this leads to a highly dispersive convection scheme with strong phase-lag errors — just as in one dimension. Cellwise quadratic interpolation (independent of velocity direction) leads to a very accurate convection-diffusion scheme with excellent phase behaviour. Under constant coefficient conditions, this is a uniformly third-order polynomial interpolation algorithm (UTOPIA). Since highly accurate solutions can be obtained on relatively coarse grids, UTOPIA is much more cost-effective than lower-order methods.

Because fluxes are estimated directly, (for a given sub-cell interpolation) the flux-integral method produces *unique* formulae for the fluxes. This is in contrast to other methods that have been used to construct *conservative* multidimensional convection (or convection-diffusion) schemes. For example, Ekebjærg and Justesen [9] developed a nominally third-order, two-dimensional convection-diffusion scheme by successive elimination of truncation error terms arising from a lower-order scheme. The nonconservative single-step explicit update was then rewritten in a conservative *pseudoflux*-difference form. But the pseudofluxes chosen by Ekebjærg and Justesen are not unique; except for first-order (and some simple second-order) schemes, there is, in general, *no unique way* of rewriting a nonconservative update in a conservative flux-difference form [4].

Recently, Rasch [10] has used, as a starting point, a (constant-coefficient) third-order semi-Lagrangian convection scheme, and then rewritten the update in conservative form. Recognising the nonuniqueness problem, Rasch uses weighting parameters to generate a family of possible pseudoflux-difference algorithms. For certain choices of the weights, the (purely convective form of the) Ekebjærg-and-Justesen scheme can be retrieved. For other weights, Rasch's convection scheme is equivalent to (the convective part of) that used by the present authors in Reference 8; this is also the form used by Rasch. For still other choices of the weights, a nominally third-order convective flux equivalent to (39) — but with the last two (higher-order) terms removed — can be obtained. The conservatively rewritten semi-Lagrangian approach does not generate diffusive fluxes.

In a very recent manuscript, LeVeque [11] has used a technique for purely convective flows similar, in some respects, to the flux-integral method described here. For a constant convecting velocity field, LeVeque's Method V is a ten-point third-order two-dimensional convection scheme. This is the minimum number of points needed for third-order accuracy. The overall convective update is equivalent to the semi-Lagrangian scheme used as the starting point for Rasch's method; it is also equivalent to that of Ekebjærg and Justesen. LeVeque's Method VI is equivalent to the purely convective portion of the flux-integral method developed here; i.e., (39). LeVeque does not consider diffusive fluxes.

For simplicity, the present paper has been confined to two dimensions. It should be clear that the flux-integral method generalises to three dimensions in a straight-forward manner. The technique can be used with even higher-order sub-cell interpolation (presumably using velocity-direction-independent interpolants in order to minimise dispersion); however, higher-order diffusive-diffusive and convective-diffusive cross-coupling terms appear to be quite complex. Further research is needed to extend the method to larger time steps. Finally, it should be pointed out that *shape preservation in the sub-cell interpolation* automatically results in a *positivity-preserving* conservative multidimensional formulation — thus obviating the need for *ad hoc* flux-limiter constraints. This is an area of current research.

REFERENCES

1. P.D. Lax and B. Wendroff, 'Systems of conservation laws', *Comm. Pure Appl. Math.*, **13**, 217-237 (1960).
2. A. Staniforth and J. Côté, 'Semi-Lagrangian integration schemes—a review', *Monthly Weather Review*, **119**, 2206-2223 (1991).
3. J.E. Fromm, 'A method for reducing dispersion in convective difference schemes', *J. Comput. Phys.*, **3**, 176-189 (1968).
4. B.P. Leonard, M.K. MacVean, and A.P. Lock, 'UTOPIA and related multidimensional unsteady convection-diffusion schemes', NASA TM****, ICOMP 94-*-*, Lewis Research Center, 1994.
5. B.P. Leonard, 'A stable and accurate convective modelling procedure based on quadratic upstream interpolation', *Comput. Methods Appl. Mech. Eng.*, **19**, 59-98 (1979).
6. B.P. Leonard, 'Elliptic systems: finite-difference method IV', in Minkowicz *et al.* (eds.), *Handbook of Numerical Heat Transfer*, Wiley, New York, Ch. 9., pp. 347-378 (1988).
7. B.P. Leonard, 'The ULTIMATE conservative difference scheme applied to unsteady one-dimensional advection', *Comp. Methods Appl. Mech. Eng.*, **88**, 17-74 (1991).

8. B.P. Leonard, M.K. MacVean and A.P. Lock, 'Positivity-preserving numerical schemes for multidimensional advection', NASA TM 106055, ICOMP-93-05, Lewis Research Center, (1993).
9. L. Ekebjærg and P. Justesen, 'An explicit scheme for advection-diffusion modelling in two dimensions', *Comput. Methods Appl. Mech. Eng.*, **88**, 287-297 (1991).
10. P.J. Rasch, 'Conservative shape-preserving two-dimensional transport on a spherical reduced grid', *Monthly Weather Review*, in press.
11. R.J. LeVeque, 'High-resolution conservative algorithms for advection in incompressible flow', *SIAM J. Numer. Anal.*, in press.

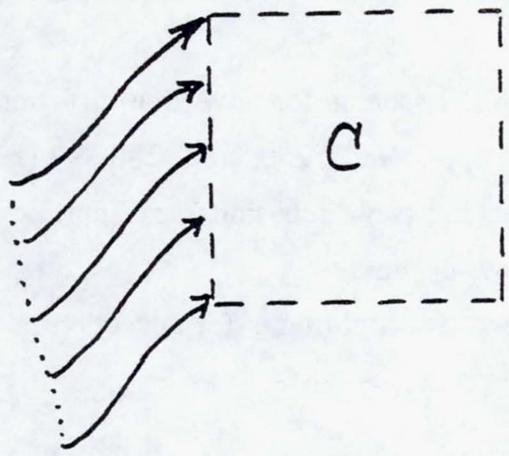

Figure 1 Schematic of particle paths flowing into the west face of cell C.

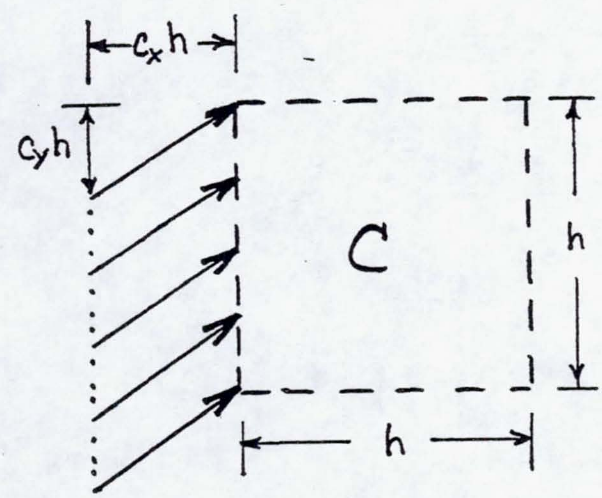

Figure 2 The flux-integral parallelogram in the vicinity of the west face of cell C; $c_{xw}, c_{yw} > 0$.

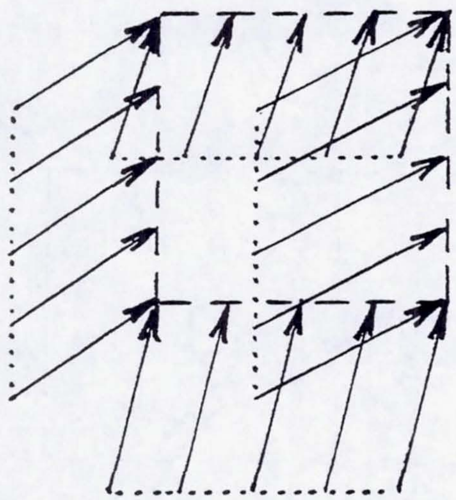

Figure 3 Flux-integral parallelograms on each face of cell C.

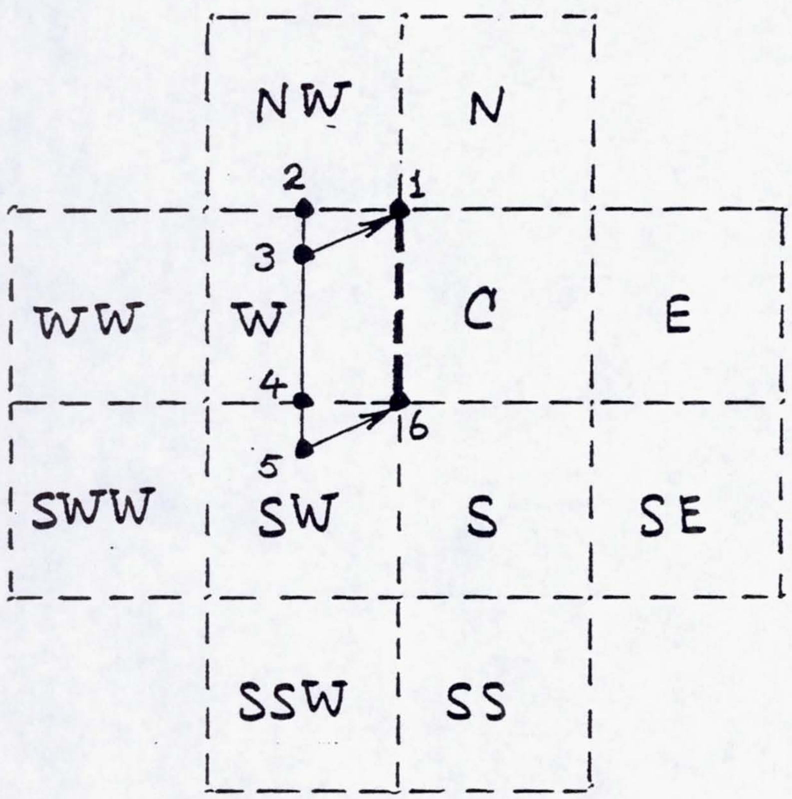

Figure 4 Twelve cells in the vicinity of the west face of cell C; c_x, $c_y > 0$.

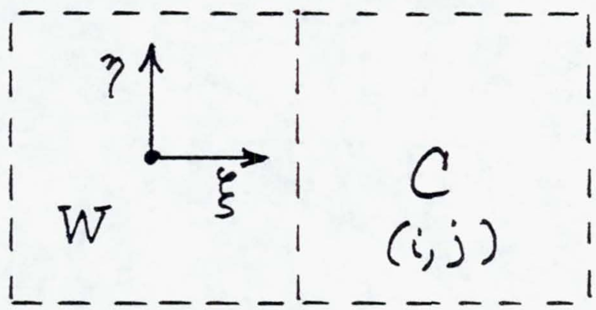

Figure 5 Definition of local normalised coordinates within cell *W*.

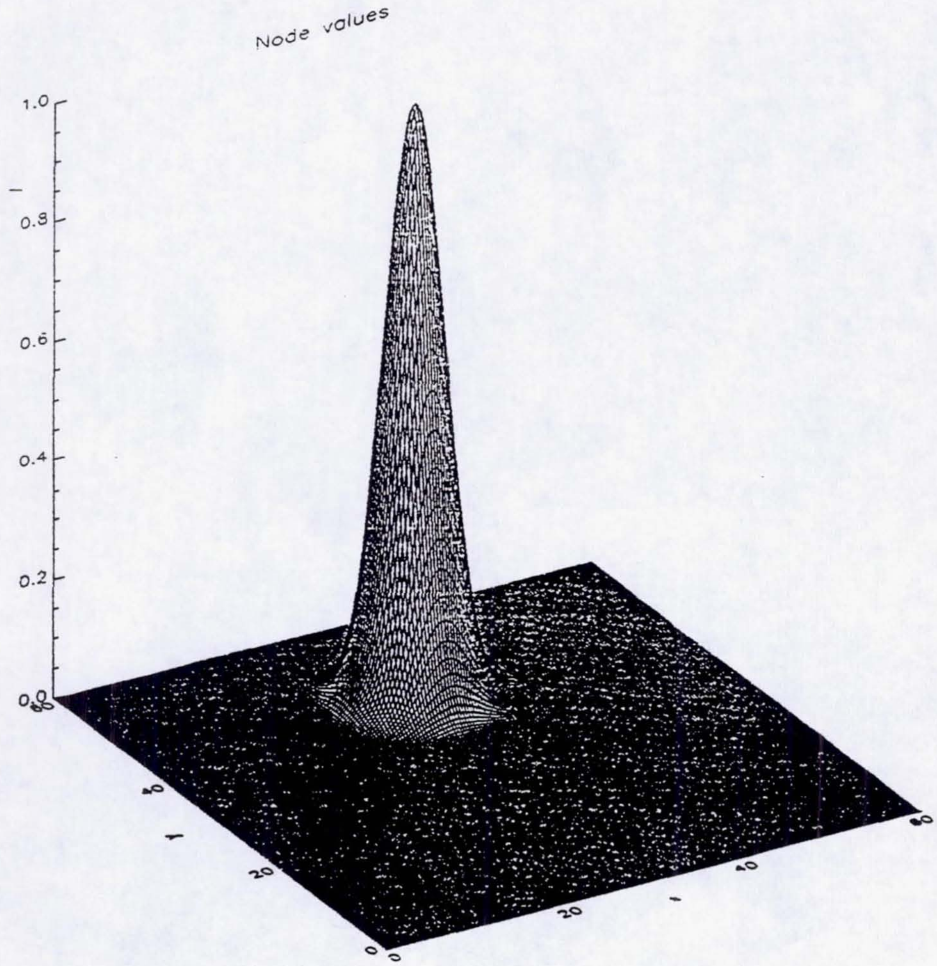

Figure 6 Initial Gaussian distribution shown on a very fine grid. This is also the exact (purely convective) solution after an integral number of rotations; $\phi_{max} = 1.000$.

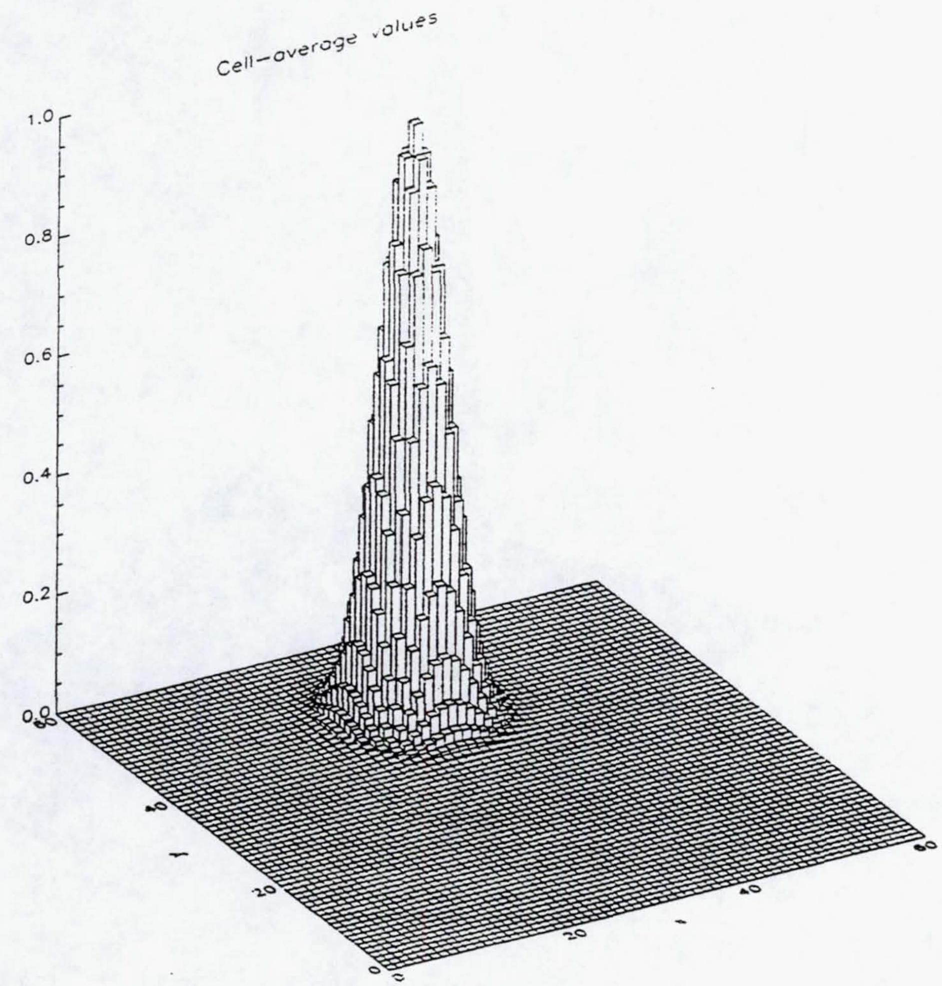

Figure 7 Initial state of cell-average values, shown as a two-dimensional histogram on the computational grid; $\bar{\phi}_{max} = 0.991$.

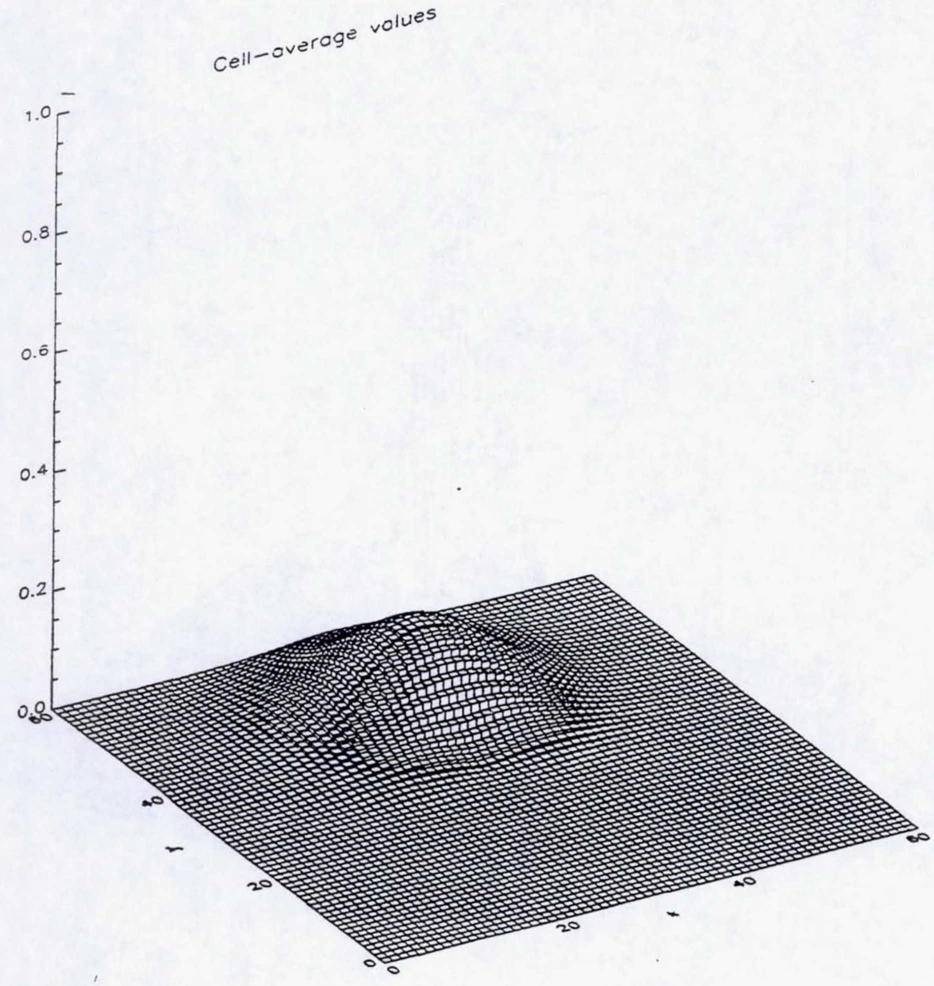

Figure 8 Solution after one (anticlockwise) rotation for the first-order method. In this case, the histogram of cell-average values also represents the cellwise constant sub-cell interpolation. $\bar{\phi}_{max} = 0.152$; $\bar{\phi}_{min} = 0.0$.

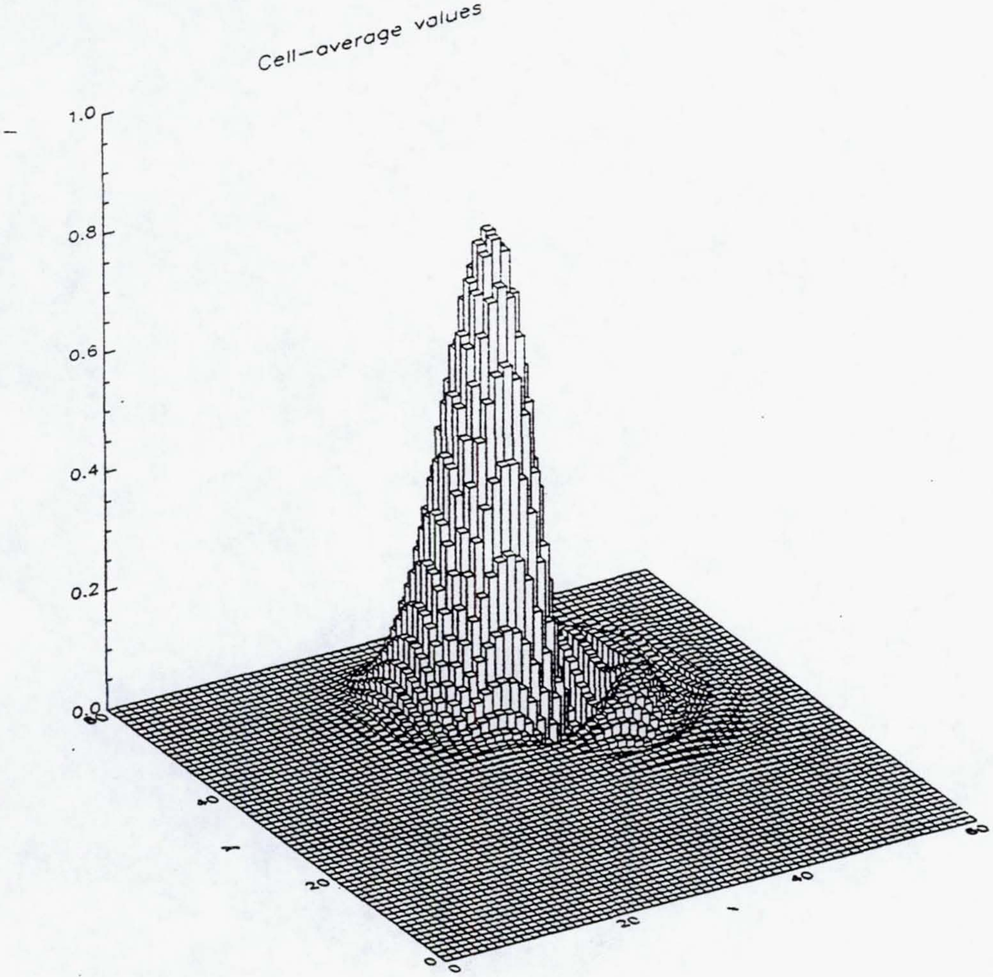

Figure 9 Solution of cell-average values after one rotation using the second-order convection scheme; $\bar{\phi}_{max} = 0.787$; $\bar{\phi}_{min} = -0.149$.

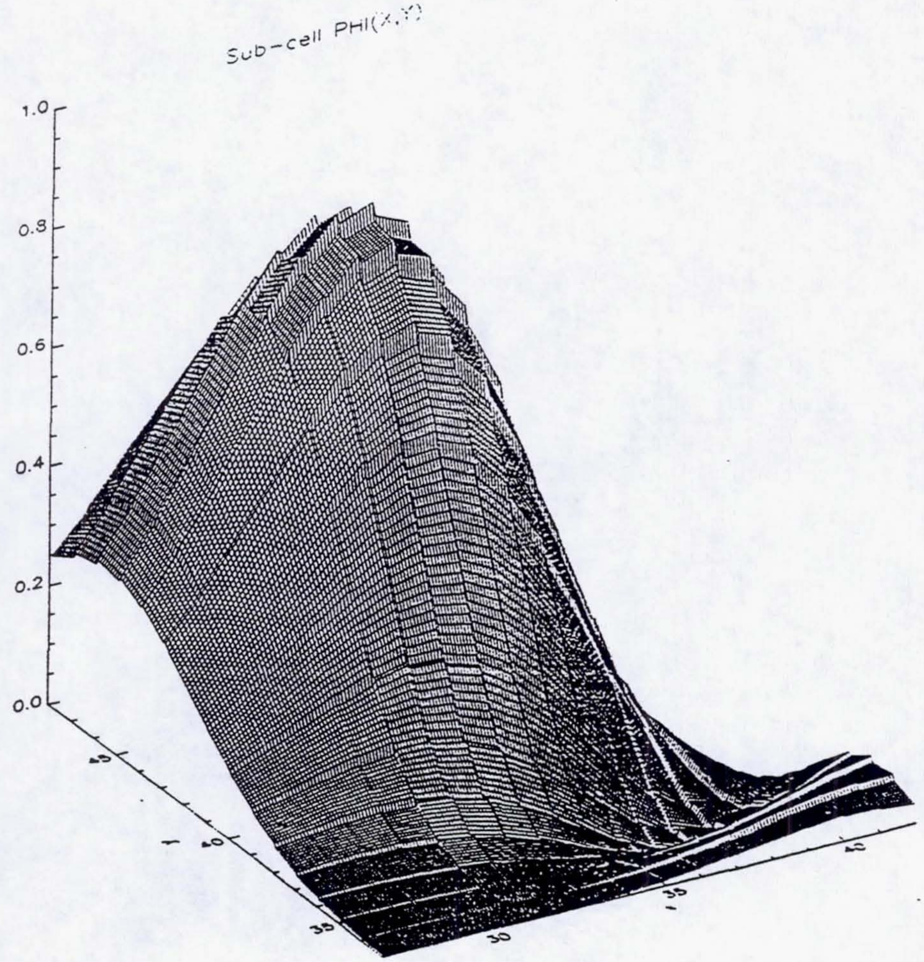

Figure 10 Close-up of the downwind-weighted bilinear sub-cell interpolation in the peak region, showing discontinuities across cell faces; $\phi_{max} = 0.823$; $\phi_{min} = -0.176$.

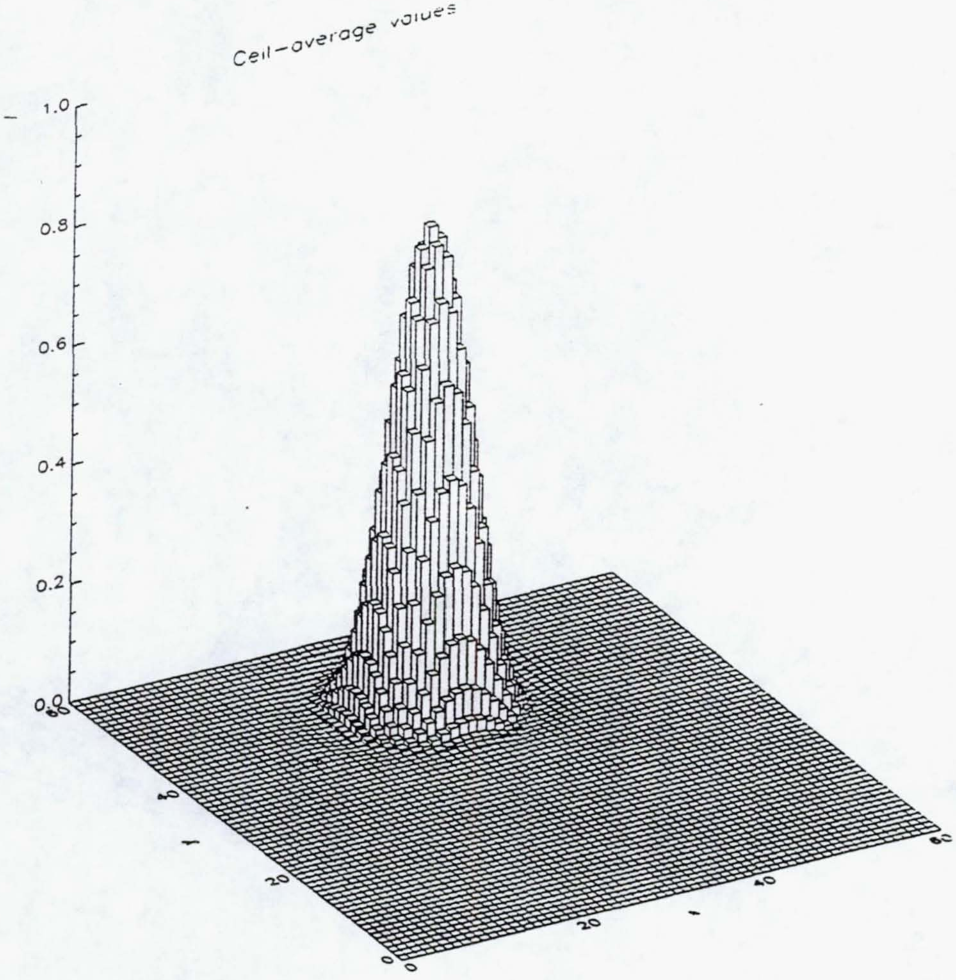

Figure 11 Solution of cell-average values after one rotation using the purely convective form of UTOPIA; $\bar{\phi}_{max} = 0.804$; $\bar{\phi}_{min} = -0.008$.

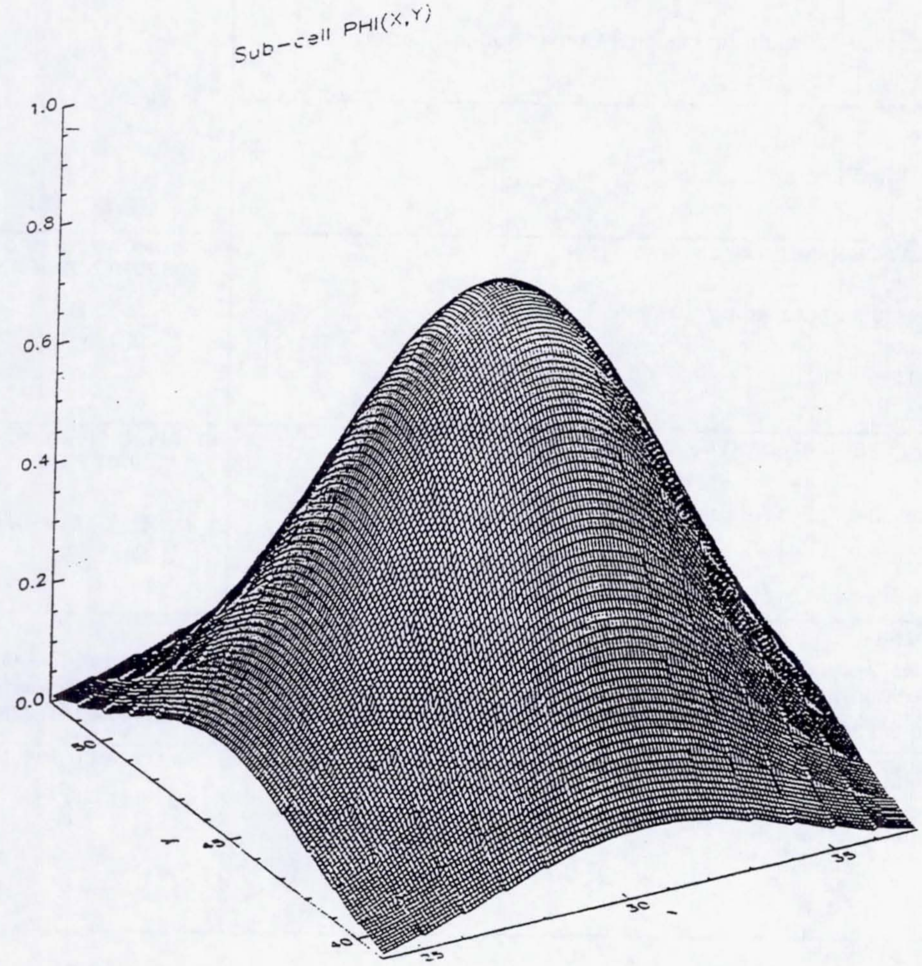

Figure 12 Close-up of the quadratic sub-cell interpolation in the peak region, showing (small) discontinuities across cell faces; ϕ_{max} = 0.810; ϕ_{min} = -0.010 (not shown).

REPORT DOCUMENTATION PAGE

Form Approved
OMB No. 0704-0188

1. AGENCY USE ONLY (*Leave blank*)	2. REPORT DATE	3. REPORT TYPE AND DATES COVERED
	August 1994	Technical Memorandum

4. TITLE AND SUBTITLE

The Flux-Integral Method for Multidimensional Convection and Diffusion

5. FUNDING NUMBERS

WU–505–90–5K

6. AUTHOR(S)

B.P. Leonard, M.K. MacVean, and A.P. Lock

7. PERFORMING ORGANIZATION NAME(S) AND ADDRESS(ES)

National Aeronautics and Space Administration
Lewis Research Center
Cleveland, Ohio 44135–3191

8. PERFORMING ORGANIZATION REPORT NUMBER

E–9019

9. SPONSORING/MONITORING AGENCY NAME(S) AND ADDRESS(ES)

National Aeronautics and Space Administration
Washington, D.C. 20546–0001

10. SPONSORING/MONITORING AGENCY REPORT NUMBER

NASA TM–106679
ICOMP–94–13

11. SUPPLEMENTARY NOTES

B.P. Leonard, Institute for Computational Mechanics in Propulsion, NASA Lewis Research Center, (work funded under NASA Cooperative Agreement NCC3–233), and University of Akron, Akron, Ohio 44325–3903; M.K. MacVean and A.P. Lock, Atmospheric Processes Research Division, Meteorological Office, Bracknell, Berkshire, RG12 2SZ, U.K. ICOMP Program Director, Louis A. Povinelli, organization code 2600, (216) 433–5818.

12a. DISTRIBUTION/AVAILABILITY STATEMENT

Unclassified - Unlimited
Subject Categories 34 and 64

12b. DISTRIBUTION CODE

13. ABSTRACT *(Maximum 200 words)*

The flux-integral method is a procedure for constructing an explicit, single-step, forward-in-time, conservative, control-volume update of the unsteady, multidimensional convection-diffusion equation. The convective-plus-diffusive flux at each face of a control-volume cell is estimated by integrating the transported variable and its face-normal derivative over the volume swept out by the convecting velocity field. This yields a *unique* description of the fluxes, whereas other conservative methods rely on nonunique, arbitrary pseudoflux-difference splitting procedures. The accuracy of the resulting scheme depends on the form of the *sub-cell interpolation* assumed, given cell-average data. Cellwise constant behavior results in a (very artificially diffusive) first-order convection scheme. Second-order convection-diffusion schemes correspond to cellwise linear (or bilinear) sub-cell interpolation. Cellwise quadratic sub-cell interpolants generate a highly accurate convection-diffusion scheme with excellent phase accuracy. Under constant-coefficient conditions, this is a uniformly third-order polynomial interpolation algorithm (UTOPIA).

14. SUBJECT TERMS

Flux-integral; Convection; Diffusion; Conservative; Multidimensional; Higher-order

15. NUMBER OF PAGES

29

16. PRICE CODE

A03

17. SECURITY CLASSIFICATION OF REPORT	18. SECURITY CLASSIFICATION OF THIS PAGE	19. SECURITY CLASSIFICATION OF ABSTRACT	20. LIMITATION OF ABSTRACT
Unclassified	Unclassified	Unclassified	